Journal of Nanofluids
Vol. 6, pp. 637–646, 2017
(www.aspbs.com/jon)

MHD Boundary Layer Flow of Nanofluid Over a Nonlinear Stretching Sheet with Effect of Non-Uniform Heat Source and Chemical Reaction

T. Srinvasulu[1,*] and Shankar Bandari[2]

[1]*Department of Mathematics, M. V. S GDC, Mahabubnagar 509001, Telangana, India*
[2]*Department of Mathematics, Osmania University, Hyderabad 500007, Telangana, India*

The aim of the present paper is to study MHD boundary layer flow of a nanofluid over a non-linear stretching sheet with the effects of non-uniform heat source and chemical reaction. The governing equations of the problem are transformed into non-linear ordinary differential equations by using similarity transformations. The resulting equations are solved numerically by using an implicit finite difference method known as Keller Box method. The effect of various physical parameters on the dimensionless velocity, dimensionless temperature and dimensionless concentration profile are showed graphically and discussed for the relative parameters. Present results are comparisons have been made with previously published work and results are found to be very good agreement. Numerical results for local skin friction, local Nusselt number and local Sherwood number are tabulated for various physical parameters.

KEYWORDS: MHD, Boundary Layer, Non-Linear Stretching Sheet, Non-Uniform Heat Source, Chemical Reaction, Suction.

1. INTRODUCTION

Nanofluid is a fluid that contains nanometer sized particles. Choi[1] is used the term nanofluid in first time. Nanofluids are more stable and sufficient viscosity. Nanoparticle material such as metallic Oxides [Al_2O_3, CuO], nitrides ceramics [AIN, SiN], carbide ceramics [SiC, TiC], etc. have been used for preparation of nanofluid. Nanofluids are used to enhance the thermal conductivity as well as heat transfer performance at low level concentration of base fluids like water. Several researchers have shown that thermal conductivity of solid metals is higher than base fluid. Convective transport in fluids was discussed by Buongiorno.[7] Khan and Pop[3] studied laminar flow of nanofluid resulting from the stretching of a flat surface by using an implicit finite difference method, which is the initial work on stretching sheet of a nanofluid. Wubshet Ibrahim and Bandari Shankar[4] investigated MHD Boundary layer flow and heat transfer of nanofluid over stretching sheet. Kalidas Das analyzed[5] Nanofluid flow over a non-linear permeable stretching sheet with partial slip and observed that nanoparticle concentration is an increasing function for the values of slip parameter and non-linear stretching parameter.

*Author to whom correspondence should be addressed.
Email: mailtsvs@gmail.com
Received: 9 December 2016
Accepted: 31 January 2017

Rana and Bhargava[6] numerically studied about the boundary layer flow of nanofluid over a non-linear stretching of a flat surface by using the finite element method. The stretching sheet problem was introduced in 1973 by Mc Coramack and Crane.[27] The steady flow over stretching sheet have many applications like non-Newtonian fluids, MHD flows, porous plate, and heat transfer analysis.[8] Zaimi et al.,[9] investigated, boundary layer flow and heat transfer of a nanofluid over a non-linear permeable stretching sheet is numerically by using shooting method.

Boundary layer flow and heat transfer over a stretching sheet in nanofluids have diverse applications in industrial, engineering and scientific problems such as micro MHD pumps, plasma studies, MHD power generators, cooling nuclear reactors and geothermal extractions. Ansari et al.[10] studied numerically boundary layer flow and heat transfer over a nonlinear permeable stretching surface with non-uniform heat generation/absorption and found their investigation, in the presence of the stronger magnetic field, the momentum boundary layer become thinner and thermal boundary layer thickness and nanoparticle volume fraction boundary layer thickness become thicker. Makinde and Aziz,[11] investigated boundary layer flow of a nanofluid past a stretching sheet with a convective boundary condition. Zaimi et al.,[12] studied boundary layer flow and heat transfer over a non-linearly permeable stretching/shrinking sheet in a nanofluid. Mahood et al.[13] are investigated numerically, MHD boundary layer flow and

ARTICLE

heat transfer of a water based nanofluid over a non-linear stretching sheet with viscous dissipation by using Runge-Kutta-Fehlberg fourth fifth order method. Ishak[14] was examined, MHD Boundary layer flow due to an Exponentially stretching sheet with Radiation effect numerically and found that the surface shear stress increased with the magnetic parameter and the heat transfer rate increases with Prandtl number, but decreases with both Magnetic parameter and radiation parameter.

Raju et al.[15] are analyzed Dual Solutions of MHD Boundary layer Flow with effect of non-uniform heat source/sink over a past an exponentially stretching sheet. Mutuku[16] was studied numerically, MHD Non-linear boundary layer flow and heat transfer of nanofluid past a permeable moving flat surface with thermal radiation and viscous dissipation. Rudraswamy and Gireesha[18] addressed, boundary layer flow and heat transfer of a nanofluid over an exponential stretching surface, in the presence of uniform thermophoresis and Brownian diffusion motion.

Gupta and Gupta[19] have studied, heat and mass transfer on a stretching sheet with suction or blowing. Magyari and Keller[20] discussed, heat and mass transfer in the boundary layers flow over an exponentially stretching continuous surface. Rao et al.,[25] numerically studied, conjugate effect of heat transfer of a nanofluid over a nonlinear stretching sheet, increasing the Brownian motion parameter and heat source/sink parameters enhances the thermal boundary layer thickness. Reddy[26] was investigated, the effect of MHD and thermal radiation of boundary layer flow of a nanofluid over stretching sheet, if increase the magneto parameter and the thermal radiation parameter then the thermal boundary layer thickness is increases.

Chemical reactions are two types namely homogeneous and heterogeneous reactions. Homogeneous reaction involves only single phase reaction, heterogeneous reaction which involves two or more phase reactions. Heat and mass transfer in a nanofluid over a stretching sheet with chemical reaction effect has many applications such as drying, groves of fruit trees, damage of crops due to freezing and energy transfer in a wet cooling tower. Kasumani et al.,[31] are investigate effect of chemical reaction on convective heat transfer of nanofluid over a wedge with heat generation in presence of suction parameter. Shehzad et al.,[32] are studied about the effect of mass transfer on MHD flow of casson fluid with chemical reaction and suction and observed the casson parameter and Hartman number have similar effects on the velocity profile. Also Prasannakumara[33] and co-authors studied the Effects of Chemical Reaction and Nonlinear Thermal Radiation on Williamson Nanofluid Slip Flow over a Stretching Sheet Embedded in a Porous Medium and Gireesha et al.,[34] studied the Thermal radiation and chemical reaction effects on boundary layer slip flow and melting heat transfer of nanofluid induced by a nonlinear stretching sheet. The present paper studies MHD boundary layer flow of a nanofluid over a non linear stretching sheet with effects of non-uniform heat source and chemical reaction.

2. MATHEMATICAL FORMULATION

Consider a two dimensional steady MHD boundary layer flow of incompressible, electrically conducting, viscous nanofluid over a nonlinear stretching sheet. The velocity of the stretching sheet is $u_w(x) = ax^n$ (where $a > 0$ is the constant acceleration parameter and n is nonlinear stretching parameter). The x-axis is taken along the nonlinear stretching sheet and y is the coordinate normal to the surface. The fluid is electrically conducting under the influence of magnetic field $B(x)$ normal to the stretching sheet. The induced magnetic field is neglected due to assume Reynolds number is small. Assume that stretching surface temperature T and the nanoparticle fraction C take constant values T_w and C_w respectively. The ambient values attained y tends infinity of T and C are denoted by T_∞ and C_∞ respectively. The thermal physical properties of the nanofluid assumed to be constant. The pressure gradient and external forces are neglected.

Under the usual boundary layer approximations, as per the assumptions made above, MHD nanofluid flow and non-uniform heat transfer with chemical reaction effects are governed by the following equations:

The continuity equation

$$\frac{\partial u}{\partial x} + \frac{\partial v}{\partial y} = 0 \tag{1}$$

The momentum equation

$$u\frac{\partial u}{\partial x} + v\frac{\partial u}{\partial y} = \nu\frac{\partial^2 u}{\partial y^2} - \sigma\frac{B^2}{\rho_f}u \tag{2}$$

The energy equation

$$u\frac{\partial T}{\partial x} + v\frac{\partial T}{\partial y} = \alpha\frac{\partial^2 T}{\partial y^2} + \tau\left[D_B\frac{\partial C}{\partial y}\frac{\partial T}{\partial y} + \frac{D_T}{T_\infty}\left(\frac{\partial T}{\partial y}\right)^2\right] + \frac{q'''}{(\rho c)_f} \tag{3}$$

The nanoparticle concentration equation

$$u\frac{\partial C}{\partial x} + v\frac{\partial C}{\partial y} = D_B\frac{\partial^2 C}{\partial y^2} + \frac{D_T}{T_\infty}\left(\frac{\partial^2 T}{\partial y^2}\right) - K(C - C_\infty) \tag{4}$$

The associated boundary conditions are[3]

$$\begin{aligned} &\text{At } y = 0; \quad u = u_w; \quad v = v_w; \quad T = T_w; \quad C = C_w \\ &\text{At } y \to \infty; \quad u \to 0; \quad T \to T_\infty; \quad C \to C_\infty \end{aligned} \tag{5}$$

Where u, v are velocity components along x-axis and y-axis respectively. α, ν, ρ, c, $(\rho c)_p$, $(\rho c)_f$, D_B, D_T and τ are Thermal diffusivity, kinematic viscosity, mass density, specific heat, effective heat capacity of the nanoparticle material, heat capacity of the fluid, Brownian diffusion coefficient, thermophoresis diffusion coefficient and

a parameter defined as the ratio of effective heat capacity of the nanoparticle material to heat capacity of the fluid respectively. $B(x)$ is the variable magnetic field and many authors[8, 10, 13] consider it is the form $B(x) = B_o x^{(n-1)/2}$. The non-uniform heat source/sink q''' is modeled as[10, 30]

$$q''' = \left(\frac{ku_w(x)}{x\nu}\right)[A^*(T_w - T_\infty)f' + B^*(T - T_\infty)] \quad (6)$$

Where k is the thermal conductivity, A^* and B^* are parameters of space dependent and temperature dependent heat generation/absorption. Both A^* and B^* positive corresponds to internal heat source and negative to internal heat sink.

Introduce the following similarity transformations

$$\eta = y\sqrt{\frac{a(n+1)}{2\nu}}x^{(n-1)/2} \quad u = ax^n f'(\eta)$$
$$v = -\sqrt{\frac{a\nu(n+1)}{2}}x^{(n-1)/2}\left[f(\eta) + \frac{n-1}{n+1}\eta f'(\eta)\right] \quad (7)$$
$$\phi(\eta) = \frac{C - C_\infty}{C_w - C_\infty} \quad \theta(\eta) = \frac{T - T_\infty}{T_w - T_\infty}$$

Where ψ denotes stream function and is defined as $u = \partial\psi/\partial y$, $v = -\partial\psi/\partial x$ and $f(\eta)$ is a dimensionless stream function, ϕ is dimensionless concentration function and θ is dimensionless temperature function and η is similarity variable. After similarity transformations, the governing Eqs. (2)–(4) are reduced as follows:

$$f''' + ff'' - \frac{2n}{n+1}(f')^2 - Mf' = 0 \quad (8)$$

$$\frac{1}{Pr}\theta'' + \theta' f + Nb\theta'\phi' + Nt(\theta')^2 + \frac{2}{n+1}A^* f' + \frac{2}{n+1}B^*\theta = 0 \quad (9)$$

$$\phi'' + Le(f\phi') + \frac{Nt}{Nb}\theta'' - R \cdot Le \cdot \phi = 0 \quad (10)$$

The associative boundary conditions becomes

$$f'(0) = 1, \quad f(0) = S, \quad \theta(0) = 1, \quad \phi(0) = 1,$$
$$f'(\infty) \to 0, \quad \theta(\infty) \to 0, \quad \phi(\infty) \to 0 \quad (11)$$

Where

$$M = \frac{2\sigma B_o^2}{\rho a(n+1)} \quad Pr = \frac{\nu}{\alpha} \quad S = \frac{v_o}{\sqrt{a\nu}}$$
$$Nb = \frac{\tau D_B(C_w - C_\infty)}{\nu} \quad Nt = \frac{\tau D_T(T_w - T_\infty)}{T_\infty\nu} \quad (12)$$
$$Le = \frac{\nu}{D_B} \quad R = \frac{2k\nu}{(n+1)ax^{(n-1)/2}} \quad \nu = \frac{k}{(\rho c)_f}$$

Here M, Pr, S, Nb, Nt, Le and R denote Magnetic parameter, Prandtl number, Suction parameter, the Brownian motion parameter, the Thermophoresis parameter, the Lewis number and Chemical parameter respectively.

The quantities of practical interest in this study, are local skin friction coefficient Cf_x, the local Nusselt number Nu_x, and local Sherwood number Sh_x which are defined as follows:

$$C_{fx} = \frac{\mu_f}{\rho u_w^2}\left(\frac{\partial u}{\partial y}\right)_{y=0}, \quad Nu_x = \frac{xq_w}{k(T_w - T_\infty)},$$
$$Sh_x = \frac{xq_m}{D_B(C_w - C_\infty)} \quad (13)$$

Where k is the thermal conductivity of the nanofluid and q_w, q_m are heat and mass fluxes at the surface respectively and define as follows

$$q_w = -\left[\frac{\partial T}{\partial y}\right]_{y=0} \quad q_m = -D_B\left[\frac{\partial C}{\partial y}\right]_{y=0} \quad (14)$$

Substituting Eqs. (7) into (13) and (14) we obtain

$$Re_x^{1/2}C_{fx} = \sqrt{\frac{n+1}{2}}f''(0),$$
$$Re_x^{-1/2}Nu_x = -\sqrt{\frac{n+1}{2}}\theta'(0), \quad (15)$$
$$Re_x^{-1/2}Sh_x = -\sqrt{\frac{n+1}{2}}\phi'(0)$$

Where $Re_x = u_w x/\nu$ is the local Reynolds number.

3. NUMERICAL METHOD

The non linear ordinary differential Eqs. (8)–(10) together with boundary conditions (11) are solved numerically by an implicit finite difference scheme namely the Keller box method as mentioned by Cebeci and Bradshaw.[26] According to Vajravelu et al.,[27] to obtain the numerical solutions, the following steps are involved in this method.

- Reduce the ordinary differential equations to a system of first order equations.
- Write the difference equations for ordinary differential equations using central differences.
- Linearize the algebraic equations by Newtons method, and write them in matrix vector form.
- Solve the linear system by the block tri-diagonal elimination technique.

The accuracy of the method is depends on the appropriate initial guesses. We made an initial guesses are as follows.

$$f_0(\eta) = (1 + S - e^{-x}), \quad \theta_0(\eta) = e^{-x}, \quad \phi_0(\eta) = e^{-x}$$

The choices of the above initial guesses depend on the convergence criteria and the transformed boundary conditions of Eqs. (10) and (11). The step size 0.06 is used to obtain the numerical solution with four decimal place accuracy as the criterion of convergence.

ARTICLE

Table I. The comparison of Nusselt number $[-\theta'(0)]$ when $Nb = Nt = R = A^* = B^* = M = Le = S = 0$ and $n = 1$.

Pr	Khan and Pop[3]	Present value
0.07	0.0633	0.0666
0.20	0.1691	0.1691
0.70	0.4539	0.4539
2.	0.9113	0.9115
7	1.8954	1.8969
20	3.3539	3.3639
70	6.4261	6.5447

4. RESULTS AND DISCUSSION

The nonlinear differential Eqs. (8)–(10) with boundary conditions (11) are solved numerically by using Implicit finite difference method, is known as Keller box method Cebeci and Bradsha,[28] vijaya laxmi and Bandari Shankar.[29] Tables I and II shows the comparison of the data produced by the present method and that Khan and Pop, Rana and Bhargava respectively. The result show excellent agreement among data.

Figure 1 shows the effect of Magnetic parameter M on the velocity profile. Increase in M, depreciates the velocity profile due to The Lorentz force. It is a resistive force which is against the flow. The Lorentz force tends to slow down the motion of the fluid in the boundary layer. Figures 2–4 shows the effect of the suction parameter S on dimensionless velocity, dimensionless temperature and nano particle volume fraction in the boundary layer. Increase in S. Due to imposition of wall suction, the fluid is brought closer to the sheet and it reduces momentum boundary layer thickness and as well as thermal and nano particle volume boundary layer thickness. These causes lead to decrease the velocity, temperature and nano particle volume fraction.

Table II. Comparison of Nusselt and Sherwood number when $Nb = Nt = 0.5$, $M = S = R = A^* = B^* = 0$ and $Le = 2$.

		$-\theta'(0)$		$-\phi'(0)$	
n	Pr	Rana and Bhargava[6]	Present result	Rana and Bhargava[6]	Present result
0.2	0.7	0.3299	0.3252	0.8132	0.8058
0.3		0.3261	0.3216	0.7965	0.7985
3		0.3059	0.298	0.763	0.7508
10		0.3002	0.2922	0.7524	0.735
20		0.2825	0.2896	1.4548	0.7336
0.2	2	0.3999	0.3989	0.8048	0.8065
0.3		0.393	0.3961	0.7826	0.7975
3		0.3786	0.3777	0.7379	0.7389
10		0.3739	0.3731	0.7238	0.7144
20		0.3726	0.371	0.7201	0.7178
0.2	7	0.2248	0.2214	1.0114	1.0156
0.3		0.2261	0.222	0.9808	1.0033
3		0.2288	0.2258	0.9185	0.9222
10		0.2297	0.2267	0.8985	0.9021
20		0.2299	0.227	0.8933	0.893

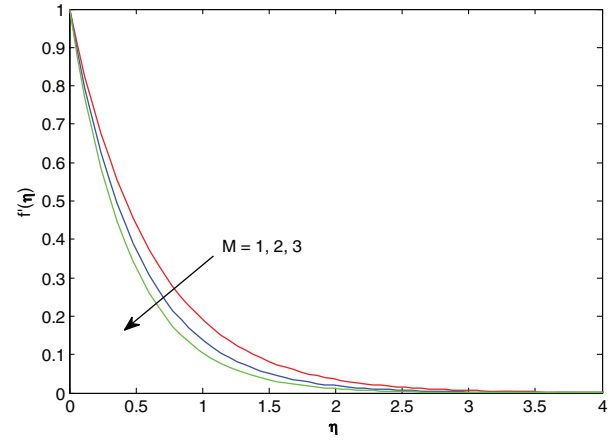

Fig. 1. Effect of magnetic parameter M on velocity profile when $Pr = Le = R = 1$, $Nb = Nt = A^* = B^* = 0.1$ and $n = S = 0.5$.

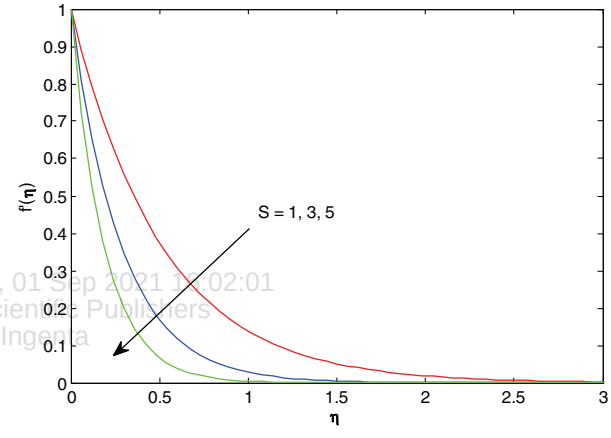

Fig. 2. Effect of suction parameter S on velocity profile when $M = Pr = Le = R = 1$, $Nb = Nt = A^* = B^* = 0.1$ and $n = 0.5$.

Figure 5 shows the effect of space dependent parameter A^* on the temperature profile. Temperature profile is increase with A^* increase. This is expected since the presence of heat source A^* in the boundary layer generates

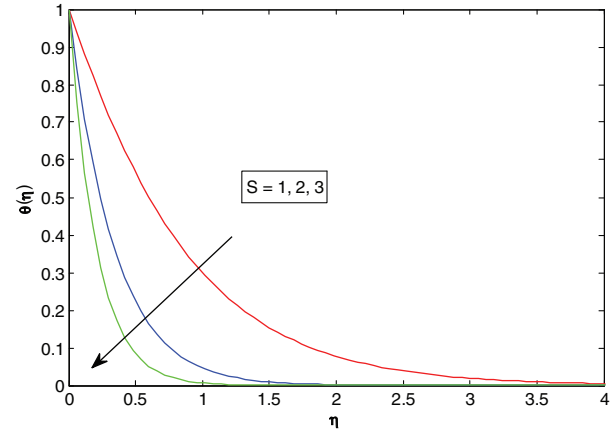

Fig. 3. Effect of suction S on temperature profile when parameter $M = Pr = Le = R = 1$, $Nb = Nt = A^* = B^* = 0.1$ and $n = 0.5$.

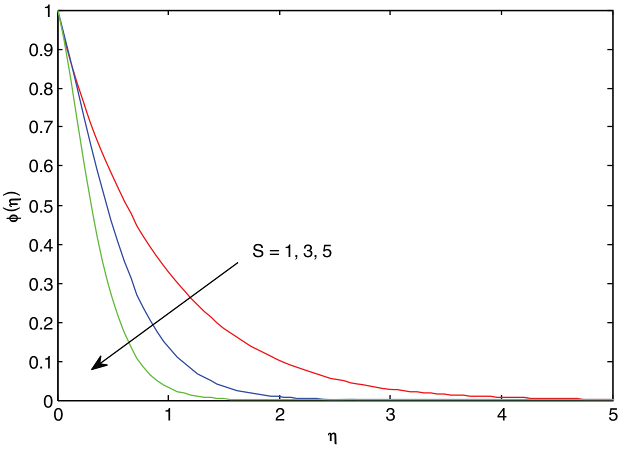

Fig. 4. Effect of suction parameter S on concentration profile when $M = Pr = Le = R = 1$, $Nb = Nt = A^* = B^* = 0.1$ and $n = 0.5$.

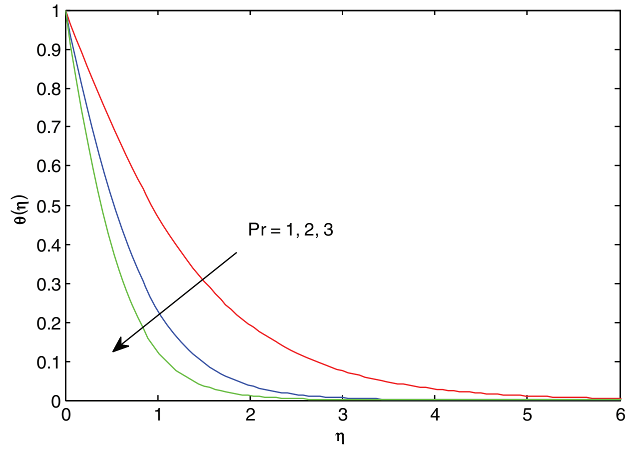

Fig. 7. Effect of Prandtl number Pr on temperature profile when $M = Le = R = 1$, $Nb = Nt = A^* = B^* = 0.1$ and $n = S = 0.5$.

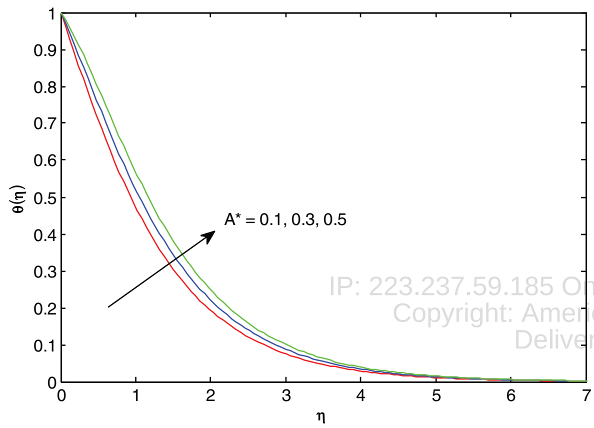

Fig. 5. Effect of space dependent parameter A^* on temperature profile when $M = Pr = Le = R = 1$, $Nb = Nt = B^* = 0.1$ and $S = n = 0.5$.

energy. This causes the temperature of the fluid to increase. Figure 6 shows the variation of chemical parameter R on the nano particle volume fraction (concentration profile). Increase chemical reaction parameter causes depreciate the concentration profile. Figure 7 shows the influence of Prandtl number Pr on the temperature profile. An increase in Pradtl number leads to the diminution in thickness of thermal boundary layer. Physically this is attributed to the fact that higher prandtl number fluid has a lower thermal conductivity.

Figure 8 shows effect of the Lewis number Le on concentration profile. The thickness of the volume fraction boundary layer decrease when volume fraction of the nano particle vary over the stretching sheet, which causes the reduced the Nusselt and Sherwood number to increase. Figures 9–10 shows that the effect of Brownian motion parameter Nb on the temperature profile and concentration profile of nano fluid across the boundary layer region respectively. The temperature in the boundary layer increases with the increase in Browanian motion parameter. As increase in Nb, due to movement of nanoparticles, results in increase the kinetic energy of the nanoparticle, thus rises the temperature. But it is reverse in the case of nano particle volume fraction profile, i.e., as the values

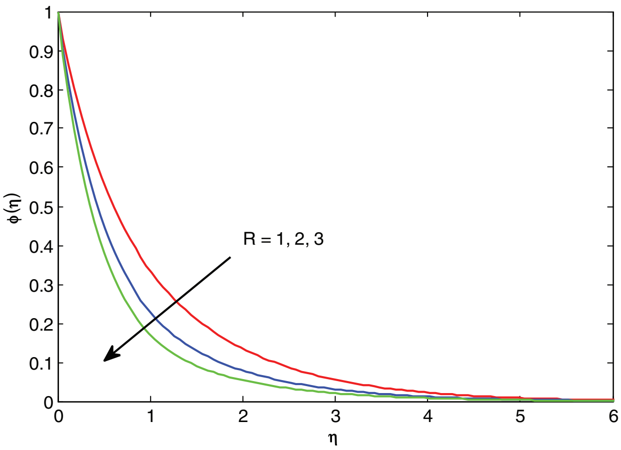

Fig. 6. Effect of chemical reaction parameter R on concentration profile when $M = Pr = Le = 1$, $Nb = Nt = A^* = B^* = 0.1$ and $n = 0.5$.

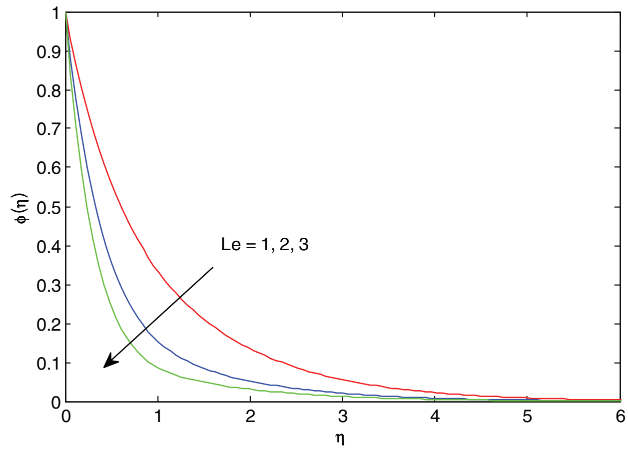

Fig. 8. Effect of Lewis number Le on concentration profile when $M = Pr = R = 1$, $Nb = Nt = A^* = B^* = 0.1$ and $n = S = 0.5$.

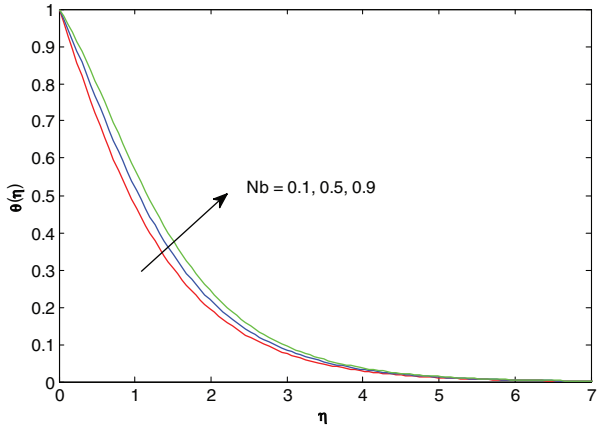

Fig. 9. Effect of Brownian motion parameter *Nb* on temperature profile when $M = Pr = Le = R = 1$, $Nt = A^* = B^* = 0.1$ and $n = S = 0.5$.

of *Nb* increase, the concentration boundary layer thickness decrease. The Brownian motion parameter increases leads to the concentration of the nanofluid decreases in the boundary layer.

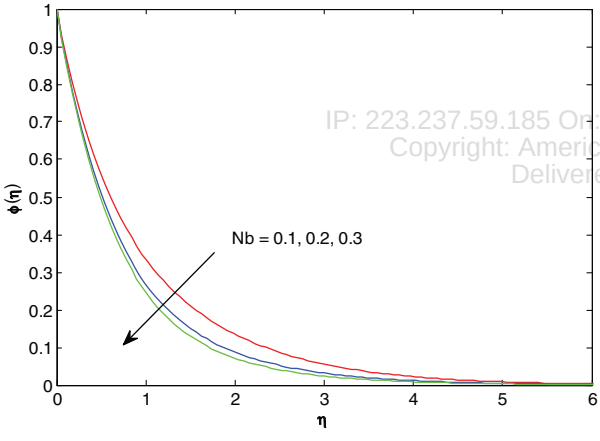

Fig. 10. Effect of Brownian motion parameter *Nb* on concentration profile when $M = Pr = Le = R = 1$, $Nt = A^* = B^* = 0.1$ and $n = S = 0.5$.

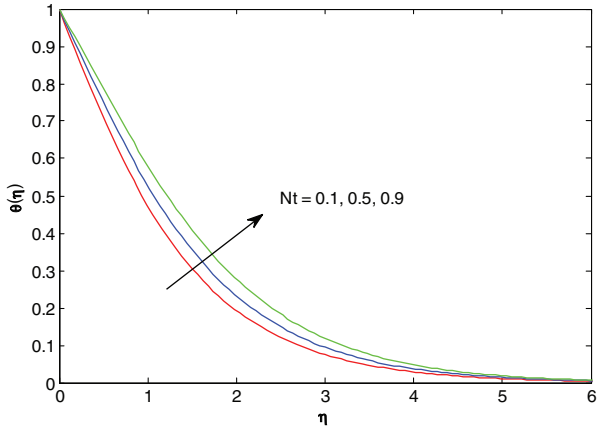

Fig. 11. Effect of Thermophoresis parameter *Nt* on temperature profile when $M = Pr = Le = R = 1$, $Nb = A^* = B^* = 0.1$ and $n = S = 0.5$.

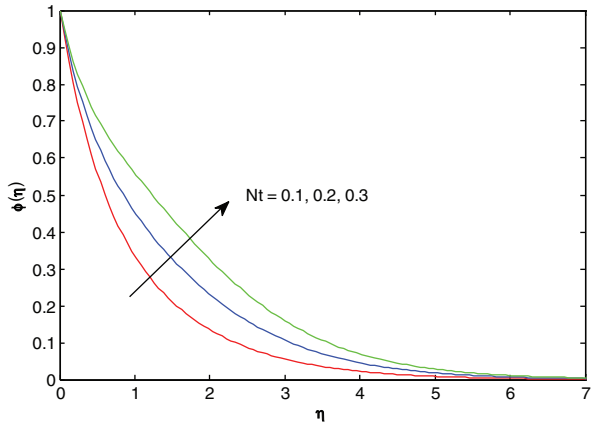

Fig. 12. Effect of Thermophoresis parameter *Nt* on concentration profile when $M = Pr = Le = R = 1$, $Nb = A^* = B^* = 0.1$ and $n = S = 0.5$.

Figures 11–12 shows the effect of Thermophoresis parameter *Nt* on dimensionless temperature and dimensionless concentration respectively. Both the dimensionless temperature and nano particle volume fraction increased

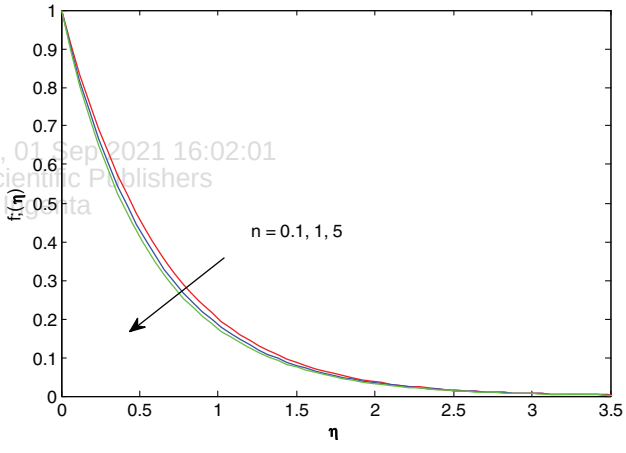

Fig. 13. Effect of non-linear stretching parameter *n* on velocity profile when $M = Pr = Le = R = 1$, $Nb = Nt = A^* = B^* = 0.1$ and $S = 0.5$.

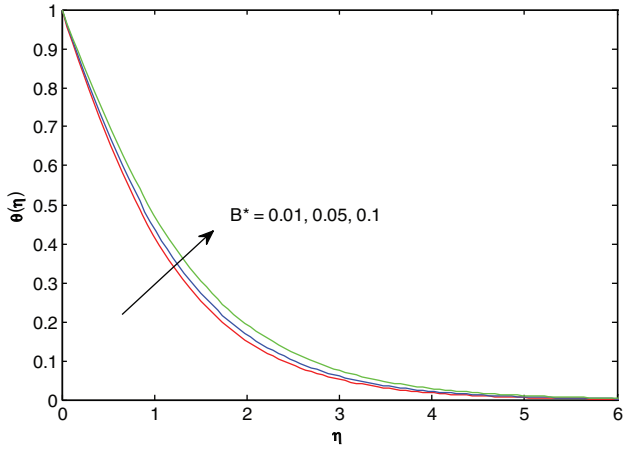

Fig. 14. Effect of temperature dependent parameter B^* on temperature profile when $M = Pr = Le = R = 1$, $Nb = Nt = A^* = 0.1$ and $S = n = 0.5$.

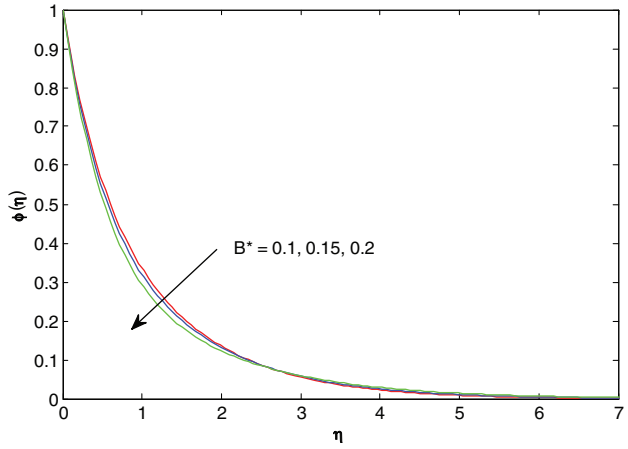

Fig. 15. Effect of temperature dependent parameter B^* on concentration profile when $M = Pr = Le = R = 1$, $Nb = Nt = A^* = 0.1$ and $S = n = 0.5$.

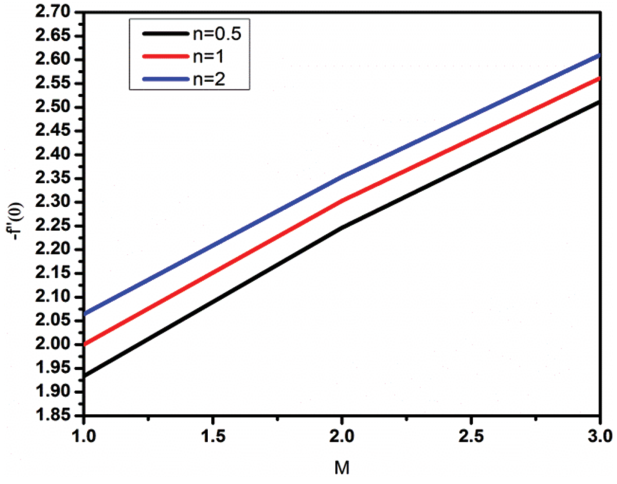

Fig. 18. Effect of n on Skin friction when $Le = Pr = R = S = 1$ and $A^* = B^* = Nb = Nt = 0.1$.

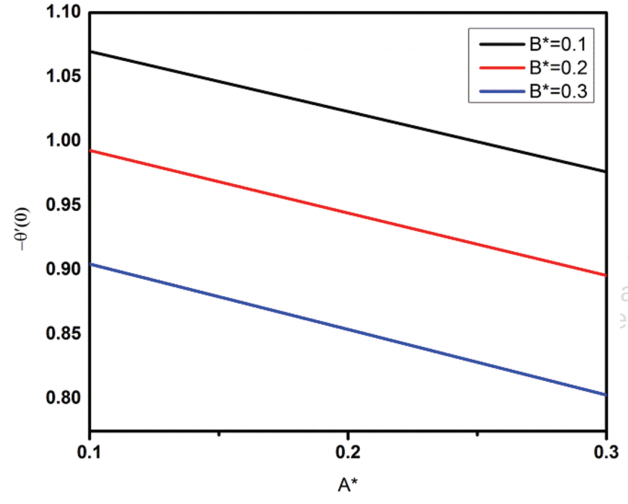

Fig. 16. Effect of B^* on Nusselt number when $M = Le = Pr = R = S = 1$, $Nb = Nt = 0.1$ and $n = 0.5$.

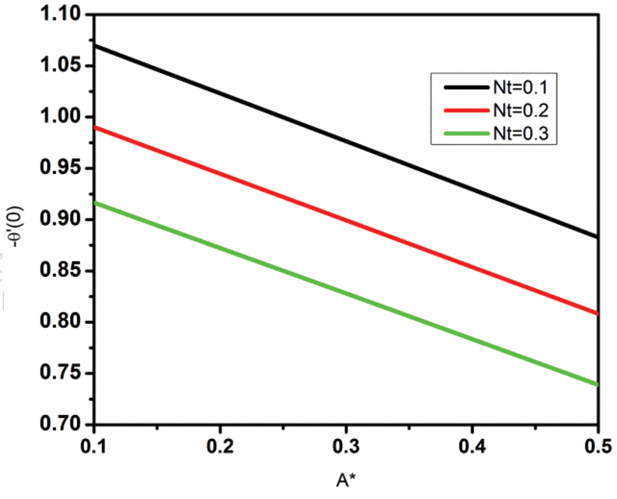

Fig. 19. Effect of Nt on Nusselt number when $M = Le = Pr = R = S = 1$, $Nb = B^* = 0.1$ and $n = 0.5$.

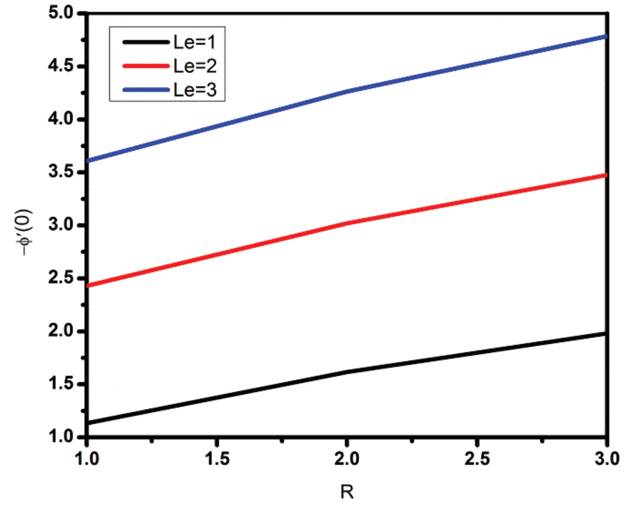

Fig. 17. Effect of Le on Sherwood number when $M = Pr = S = 1$, $A^* = B^* = Nb = Nt = 0.1$ and $n = 0.5$.

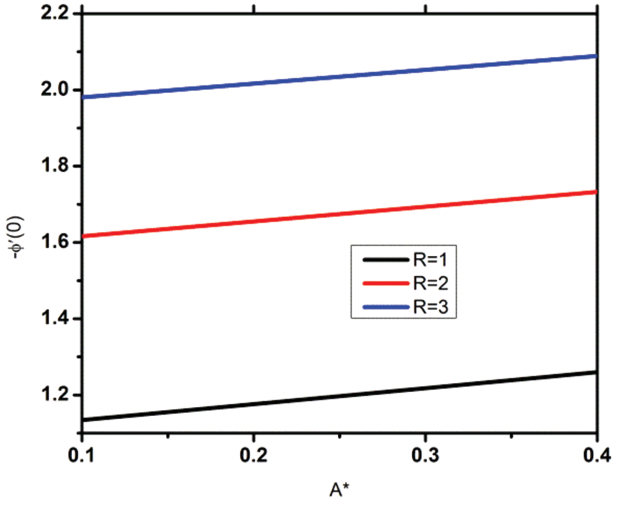

Fig. 20. Effect of R on Sherwood number when $M = Le = Pr = S = 1$, $Nb = Nt = B^* = 0.1$ and $n = 0.5$.

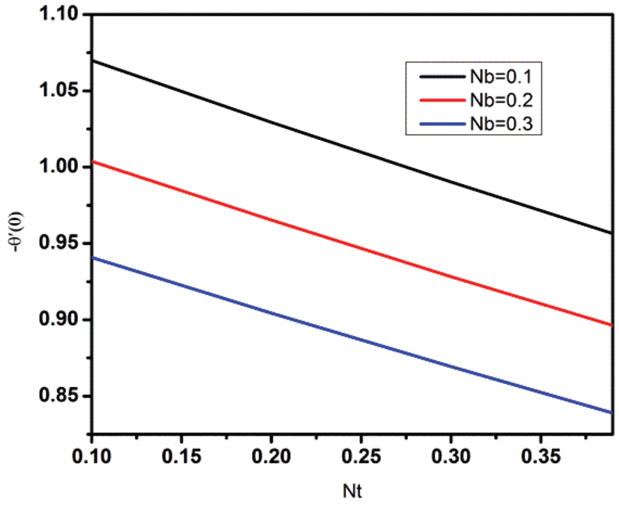

Fig. 21. Effect of Nb on Nusselt number when $M = Le = Pr = R = S = 1$, $A^* = B^* = 0.1$ and $n = 0.5$.

with *Nt* increases. This is due to fact that thermophoresis force generated by temperature gradient creates a fast flow away from the stretching surface. In this way more heated fluid is moved away from the surface and consequently as *Nt* increases, the temperature within the boundary layer increases. The fast flow from the stretching sheet carries with it thermophoretic force leads to an increase in the concentration boundary layer thickness. Figure 13 shows the influence of nonlinear stretching parameter *n* on velocity of nanofluid. Increasing the value of n leads to decrease the velocity of the nanofluid. Figures 14–15 shows that the effect of temperature dependent parameter on temperature and concentration profile respectively. Temperature profile increases and concentration profile decrease with temperature dependent parameter values increase.

Figure 16 shows the effect of A^* and B^* on Nusselt number. Rate of heat transfer increases with decrease of the values of B^*. Figure 17 shows the variation of *Le* and *R* on Sherwood number. Rate of mass transfer increases with increase of the values of *Le*. Figure 18 shows the effect of nonlinear stretching parameter and magnetic parameter on Skin friction coefficient. Rate of velocity increase with the values of *n* are increase. Figure 19 shows the effect of A^* and Nt on Nusselt number. Heat transfer rate increase with Nt decrease. Figure 20 shows the effect of A^* and *R* on Sherwood number. Mass transfer rate increases with the values of *R* increase. Figure 21 shows the effect of *Nt* and *Nb* on Nusselt number. Heat transfer rate increases with the values of *Nb* decrease.

Table III shows the variation of Skin friction coefficient $-f''(0)$, Nusselt number $-\theta'(0)$ and Sherwood number $-\phi'(0)$ for various values of parameters M, Pr, Le, Nb, Nt, S, R, A^*, B^* and n. Nusselt number and Sherwood

Table III. Numerical values of skin friction, Nusselt number and Sherwood number for various values of various parameters.

P_r	*Nb*	*Nt*	A^*	B^*	L_e	*R*	*M*	*S*	*n*	Skin friction	Nusselt number	Sherwood number
1	0.1	0.1	0.1	0.1	1	1	1	1	0.5	1.9335	1.0295	1.1696
2										1.9335	1.9074	0.3896
	0.1	0.1	0.1	0.1	1	1	1	1	0.5	1.9335	1.0295	1.1696
1	0.2									1.9335	0.9643	1.5092
	0.3									1.9335	0.9021	1.6214
	0.1	0.1								1.9335	1.0295	1.1696
		0.2								1.9335	0.9891	0.6204
		0.3								1.9335	0.9502	0.1380
		0.1	0.1							1.9335	1.0295	1.1696
			0.2							1.9335	0.9664	1.2262
			0.3							1.9335	0.9033	1.2828
			0.1	0.1						1.9335	1.0295	1.1696
				0.2						1.9335	0.9192	1.2644
				0.3						1.9335	0.7798	1.3820
				0.1	1					1.9335	1.0295	1.1696
					2					1.9335	1.0129	2.4635
					3					1.9335	1.0050	3.6390
					1	1				1.9335	1.0295	1.1696
						2				1.9335	1.0220	1.6486
						3				1.9335	1.0173	2.0101
						1	1			1.9335	1.0295	1.1696
							2			2.2464	1.0115	1.1698
							3			2.5117	0.9973	1.1707
							1	1		1.9335	1.0295	1.1696
								2		2.2785	1.9182	1.0296
								3		3.5183	2.8262	0.9165
								1	0.5	1.9335	1.0295	1.1696
									1	2	1.0672	1.1343
									1.5	2.0388	1.0892	1.1134

number are generally used as the heat transfer rate and mass transfer rate at the surface of stretching sheet respectively. Skin friction coefficient values are increases with the values of magnetic parameter, suction parameter, and nonlinear stretching parameter are increases.

5. CONCLUSIONS

In the present numerical study, MHD boundary layer flow of a nanofluid over a non-linear stretching sheet with effect of non uniform heat source and chemical reaction. The governing partial differential equations are transformed into ordinary differential equations by using a similarity transformations, which are then solved numerically using implicit finite difference method. The effect of various governing parameters namely suction parameter, nonlinear stretching parameter, chemical reaction parameter, Brownian motion parameter, thermophoresis parameter, Prandtl number and Lewis number on the velocity, temperature and concentration profile are shown graphically, presented and discussed. Numerical results for the skin friction, local Nussselt number and local Sherwood number are presented in tabular form. The main observation of the present study is as follows.

- Nusselt number increase when Pr, increase while Nusselt number decrease when Nb, Nt, A^*, B^*, Le, R and M increase.
- Sherwood number increases when Nb, Le, R and S increase, while decrease when Pr and Nt increase.
- Skin friction coefficient increase when M, S increase.
- Temperature profile increases with increase the values of M, Nt, Nb, A^*, B^* and R.
- Concentration profile increases when the values of M, Nt and n increase.
- Velocity profile decreases when M, n increase.

Nomenclature

a	Constant acceleration parameter
n	Nonlinear stretching parameter
$B(x)$	Magnetic field
T	Temperature of the fluid in the boundary layer
C	Concentration of the fluid in the boundary layer
T_w	Stretching surface temperature
C_w	Stretching surface concentration
T_∞	Ambient fluid temperature
C_∞	Ambient fluid concentration
u	Velocity component along x-axis
v	Velocity component along y-axis
u_w	Velocity component at the wall
v_w	Velocity component at the wall
υ	Kinematic viscosity
σ	Density of fluid
α	Thermal diffusivity
τ	Ratio of effective heat capacity of the nanoparticle material to heat capacity of the fluid
D_B	Brownian diffusion coefficient
D_T	Thermophoresis diffusion coefficient
k	Thermal conductivity
A^*	Space dependent parameter
B^*	Temperature dependent parameter
M	Magnetic parameter
Pr	Prandtl number
Nb	Brownian motion parameter
Nt	Thermophoresis parameter
Le	Lewis number
R	Chemical parameter
S	Suction parameter
Cf_x	Local skin friction coefficient
Nu_x	Local Nusselt number
Sh_x	Local Sherwood number.

Acknowledgments: The author T. Srinivasulu wishes to express their thanks to University Grants Commission (UGC), India, for awarding Faculty Development Programme (FDP).

References and Notes

1. S. U. S. Cho, *The Proceedings of the 1995 ASME International Mechanical Engineering Congress and Exposition*, San Francisco, USA **(1995)** p. 99, ASME, FED 231/MD 66.
2. S. U. S. Choi, Z. G. Zhang, W. Yu, F. E. Lockwood, and E. A. Grulke, *Appl. Phys. Lett.* 79, 2252 **(2001)**.
3. W. A. Khan and I. Pop, *Int. J. Heat Mass Trans.* 53, 2477 **(2010)**.
4. W. Ibrahim and B. Shankar, *Computers and Fluids* 75, 1 **(2013)**.
5. Kalidas Das, *Journal of Egyptian Mathematical Society* 23, 451 **(2015)**
6. P. Rana, and R. Bhargava, *Commun. Sci. Numer. Simulat.* 17, 212 **(2012)**.
7. J. Buongiorno, *ASME J. Heat Transfer* 128, 240 **(2006)**
8. Satish V. Desale and V. H. Pradhan, IJRET, 02, eISSN:2319/plSSN2321 **(2013)**.
9. K. Zaimi, Anuar Ishak, and L. Pop, Science reports|4:4404| DOI:10.1038/srep04404 **(2014)**.
10. Md. Ansari, R. Nandkeolyer, and S. S. Mosta, *The 6th International Conference on Computational Methods*, School of Mathematic, Statistics and Computer Science, University of Kwa-Zulu-Natal, Pietermaritzburg, South Africa **(2015)**.
11. O. D. Makinde and A. Aziz, *Int. J. Therm. Sci.* 50, 1326 **(2011)**.
12. K. Zaimi, A. Ishak, and I. Pop, *Sci. Rep.* 4, 4404 **(2014)**.
13. F. Mahood, W. A. Khan, and A. I. M. Ismail, *Journal of Magnetism and Magnetic Materials* 374, 569 **(2015)**.
14. Anuar Ishak, *Sains Malaysiana* 40, 391 **(2011)**.
15. C. S. K. Raju, N. Sandeep, C. Sulochana, and M. Jayachandra Babu, *Journal of Applied Fluid Mechanics* 9, 555 **(2016)**; W. N. Mutuku, *Universal Journal of Fluid Mechanics* 2, 55 **(2014)**.
16. W. N. Mutuku, *Universal Journal of Fluid Mechanics* 2, 55 **(2014)**.
17. Lazarus Godson Asirvatham, Journal of Thermal Engineering Yildiz Technical University Press, Istanbul, Turkey **(2015)**, Vol. 1, p. 113.
18. N. G. Rudraswamy and B. J. Gireesha, *Journal of Applied Mathematics and Physics* 2, 24 **(2014)**.
19. P. S. Gupta and A. S. Gupta, *The Canadian Journal of Chemical Engineering* 55, 744 **(1997)**.
20. E. Magyari and B. Keller, *Journal of Physics D*: *Applied Physics* 32, 577 **(1999)**.
21. N. Bachok, A. Ishak, and I. Pop, *Sci.* 49, 1663 **(2010)**.
22. A. V. Kuznetsov and D. A. Nield, *Porous Media* 85, 941 **(2010)**.

ARTICLE

23. H. Masuda, A. Ebata, K. Teramae, and N. Hishinuma, *Netsu Bussei* 7, 227 **(1993)**.
24. H. Dessie and N. Kishan, *International Journal of Engineering Research in Africa* 14, 1 **(2015)**.
25. Thommaamndru Ranga Rao, Kotha Gangadhar, B. Hema Sundar Raju, and M. Venkata Subba Rao, *Pelagia Research Library, Advances in Applied Science Research* 5, 114 **(2014)**.
26. M. G. Reddy, *J. Sci. Res.* 6, 257 **(2014)**.
27. L. J. Crane, *J. Appl. Mat. Phys. (ZAMP)* 21, 645 **(1970)**.
28. T. Cebeci and P. Bradshaw, Physical and Computational Aspect of Convective Heat Transfer, Springer-Verlag, New York **(1984)**.
29. T. Vijaya Laxmi and Bandari Shanker, *J. Nanofluids* 5, 1 **(2016)**.
30. N. Sandeep and C. Sulochana, *Engineering Science and Technology an International Journal* 18, 738 **(2015)**.
31. R. M. Kasamani, S. Sivasankaran, M. Bhuvaneswari, and Z. Siri, *Journal of Applied Fluid Mechanics* 9, 379 **(2016)**.
32. S. A. Shehzad, T. Hayat, M. Qasim, and S. Asghar, *Brazilian Journal of Chemical Engineering* 30, 187 **(2013)**.
33. B. C. Prasannakumara, B. J. Gireesha, Rama S. R. Gorla, and M. R. Krishnamurthy, *J. Aerosp. Eng.* 04016019 **(2016)**.
34. M. R. Krishnamurthy, B. C. Prasnnakumara, and Rama Subba Reddy, *Nonlinearing Engineering* **(2016)**, DOI: 10.1515/nleng-0013.